

Supplemental Information for:

**Broadband Ion Mobility Deconvolution for Rapid Analysis of Complex Mixtures**

Michael E. Pettit<sup>1</sup>, Matthew R. Brantley<sup>1</sup>, Fabrizio Donnarumma<sup>2</sup>, Kermit K. Murray<sup>2</sup>, and  
Touradj Solouki<sup>1\*</sup>

<sup>1</sup>Department of Chemistry and Biochemistry, Baylor University, Waco, TX 76798, USA

<sup>2</sup>Department of Chemistry, Louisiana State University, Baton Rouge, LA 70803, USA

**Keywords:** broadband deconvolution, co-elution, ion mobility, mass spectrometry (MS), resolving power

\*Please address reprint requests to: Professor Touradj Solouki, Department of Chemistry and Biochemistry, Baylor University Sciences Building, One Bear Place #97348, Waco, TX 76798 Telephone number: 254-710-2678, E-mail: [Touradj\\_Solouki@baylor.edu](mailto:Touradj_Solouki@baylor.edu)

**Table S1.** Experimental parameters used in this study. Please note that the gas pressures (\*) reported in Table S1 are direct instrument readouts and have not been corrected for geometry<sup>88</sup> or chemical sensitivity<sup>89</sup> factors. Factory-set default settings were used for all parameters related to ion transmission.

Parameter	Value
ESI flow rate (uL/min)	0.5
ESI voltage (kV)	3.5
Source temperature (°C)	150
Sampling cone voltage (V)	30
Source offset voltage (V)	0
Trap cell pressure (bar)*	$\sim 1.43 \times 10^{-5}$
Transfer cell pressure (bar)*	$\sim 1.73 \times 10^{-5}$
Helium cell pressure (bar)*	$\sim 1.36$
IM cell pressure (bar)*	$\sim 3.61 \times 10^{-3}$

### Differences in Pre-IM/CID between [MGRYGF + 2H]<sup>2+</sup> and [FRMYGG + 2H]<sup>2+</sup>

Differences in the degree of (a) unintentional pre-IM dissociation of isomers and (b) alkali metal adduct formation can influence the observed relative intensities of IM deconvoluted isomers. In other words, anything that can reduce the relative abundance of intact molecular ions reaching to the IM cell should reduce their corresponding deconvoluted IM peak intensities. For example, if two isomers are mixed at equimolar concentrations, the isomer that forms a higher total number of alkali metal adducts and/or dissociates more easily (*i.e.*, unintentionally dissociates prior to reaching the IM cell) should exhibit a *lower* relative intensity for its intact molecular ion upon IM deconvolution. Under our experimental conditions (*i.e.*, instrument parameter settings such as the ion acceleration voltage, ion isolation settings, background pressure, *etc.* used to acquire the data in Figure S1), unintentional pre-IM dissociation of the FRMYGG isomer was greater than the MGRYGF isomer. Furthermore, a higher total number of alkali metal adducts (for both sodium and potassium) were observed for FRMYGG than MGRYGF. Total ion mobiligrams and averaged extracted mass spectra (XMS) are represented in Figure S1 for pure MGRYGF (Figures S1a and S1b) and pure FRMYGG (Figures S1c and S1d) sample solutions. The yellow rectangles in Figures S1a and S1c are used to highlight the IM AT region from 2.08 ms to 3.18 ms that contained the doubly-charged hexapeptide ions; MS data corresponding to highlighted IM regions in Figures S1a and S1c were averaged to generate the XMS displayed in Figures S1b and S1d, respectively.

For the pure MGRYGF sample, the most abundant IM peak in the low collision-energy mobiligram (Figure S1a; orange) had an IM AT of 2.56 ms and corresponded to the doubly-charged peptide ion  $[\text{MGRYGF} + 2\text{H}]^{2+}$  (*i.e.*,  $[\text{M} + 2\text{H}]^{2+}$  in Figure S1a). IM peaks corresponding to unintentional pre-IM dissociation product ions of MGRYGF were also observed at IM ATs of 4.78 ms for  $[\text{a}_4]^+$  and  $[\text{b}_4]^+$  ions and 5.47 ms for  $[\text{y}_4]^+$ ,  $[\text{b}_5]^+$ , and  $[\text{y}_5]^+$  ions. The IM peak at 6.93 ms corresponded to the singly-charged peptide ion  $[\text{MGRYGF} + \text{H}]^+$  at  $m/z$  730. As shown in the averaged XMS displayed in Figure S1b, the doubly-charged MGRYGF peptide ion and its doubly-charged metal-adducts (*i.e.*, Na- and K-adducts) corresponded to the IM AT region 2.08 ms to 3.18 ms in Figure S1a; a neutral-loss ion (*viz.*,  $[\text{M} - \text{NH}_3 + 2\text{H}]^{2+}$ ) and an unassigned doubly-charged ion (*viz.*, at  $m/z$  341.66) were also observed in this IM AT region.

Similarly, the base IM peak in the low collision-energy mobiligram of the pure FRMYGG sample (Figure S1c, purple) had an IM AT of 2.56 ms and corresponded to the doubly-charged peptide ion  $[\text{FRMYGG} + 2\text{H}]^{2+}$  (*i.e.*,  $[\text{M} + 2\text{H}]^{2+}$  in Figure S1c). IM peaks corresponding to unintentional pre-IM dissociation product ions of FRMYGG were also observed at IM ATs of 3.05 ms for  $[\text{b}_2]^+$ ,  $[\text{b}_2 - \text{NH}_3]^+$ , and  $[\text{y}_3]^+$  ions, 4.43 ms for  $[\text{b}_3]^+$  ions, 5.54 ms for  $[\text{y}_5]^+$  and  $[\text{b}_4]^+$  ions, 6.23 ms for  $[\text{a}_4]^+$  and  $[\text{b}_5]^+$  ions, and 6.79 ms for singly-charged  $[\text{FRMYGG} + \text{H}]^+$ . As shown in the averaged XMS displayed in Figure S1d, the doubly-charged FRMYGG and its doubly-charged metal-adducts (*i.e.*, Na- and K-adducts) corresponded to the IM AT region 2.08 ms to 3.18 ms in Figure S1c; three singly-charged product ions of FRMYGG (*viz.*,  $[\text{y}_3]^+$ ,  $[\text{b}_2]^+$ , and  $[\text{b}_2 - \text{NH}_3]^+$  (not labeled in Figure S1d)), three doubly-charged product ions of FRMYGG (*viz.*,  $[\text{a}_4]^{2+}$ ,  $[\text{a}_5]^{2+}$ ,  $[\text{b}_5]^{2+}$ ), and three unassigned singly-charged ions (*viz.*, at  $m/z$  256.97, 396.62, and 403.61) were also observed in this IM AT region.

Comparison of low collision-energy broadband mobiligrams (Figures S1a and S1c) and averaged XMS (Figures S1b and S1d) of the two pure hexapeptide sample solutions confirmed that the FRMYGG peptide ion exhibited a higher degree of unintentional pre-IM/CID and metal-adduct formation than its MGRYGF counterpart peptide ion. Our deconvolution results (Figures 2a and 6a) and observed pure SIM profiles (Figures 2d and 6d) are consistent with the concept of metal-adduct formation and pre-IM dissociation (as discussed above with Figure S1) influencing the observed relative abundance of deconvoluted IM peaks (*i.e.*, intensity of the deconvoluted  $[\text{FRMYGG} + 2\text{H}]^{2+}$  IM peak is  $0.75 \pm 0.46$  times that of  $[\text{MGRYGF} + 2\text{H}]^{2+}$  counterpart in Figure 2a).

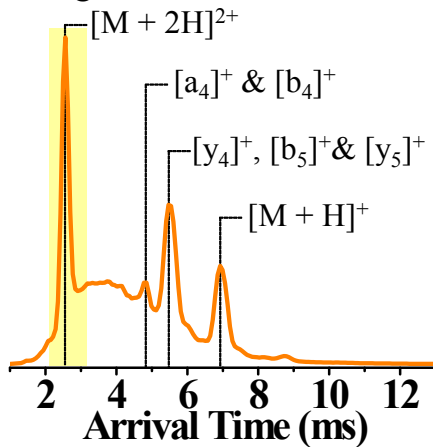
The pure SIM profile of FRMYGG (purple trace in Figure 2d) had an observable base IM peak at  $\sim 2.45$  ms and a second, less intense IM peak at  $\sim 2.91$  ms; this smaller IM peak corresponds to pre-IM dissociation products of the FRMYGG peptide ion. In this study, all high collision-energy broadband SIM profiles were generated by summing the IM data corresponding to the top 10 most abundant post-IM/CID ions in the corresponding pure isomer's CID mass spectrum. Two of the top 10 most abundant post-IM/CID product ions (*i.e.*,  $[\text{b}_2 - \text{NH}_3]^+$  and  $[\text{b}_2]^+$ ) that were used to generate the pure SIM profile of FRMYGG were also unintentionally generated prior to entering the IM cell. Therefore, the pure SIM profile of FRMYGG in Figure 2d includes IM peaks at  $\sim 2.45$

ms and ~2.91 ms because the IM data corresponding to the  $[b_2 - \text{NH}_3]^+$  and  $[b_2]^+$  fragment ions of FRMYGG included ion populations from both intentional post-IM/CID (IM ATs of ~2.45 ms) and unintentional pre-IM dissociation (IM ATs of ~2.91 ms). Similarly, the smaller IM peak in Figure 6d was characterized as belonging to unintentional pre-IM dissociation of FRMYGG ions.

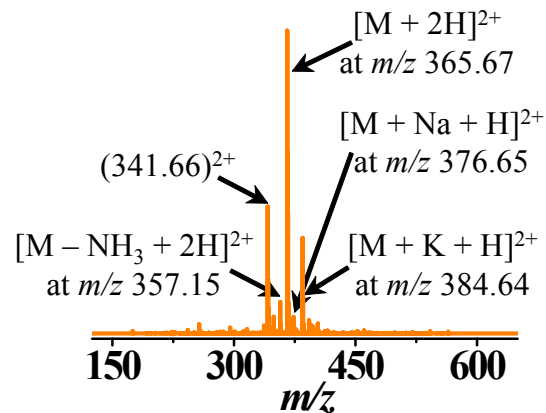
## Preparation of Biological Samples

Biological sample preparation was performed at Louisiana State University and all MS experiments and data processing were carried out at Baylor University. Trimethamine (tris) base

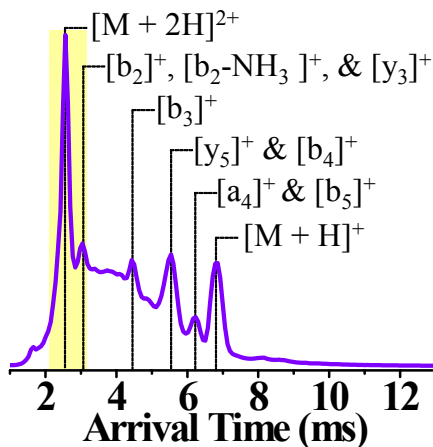
**a)** Mobiligram of Pure MGRYGF



**b)** Averaged XMS: 2.08 ms to 3.18 ms



**c)** Mobiligram Pure FRMYGG



**d)** Averaged XMS: 2.08 ms to 3.18 ms

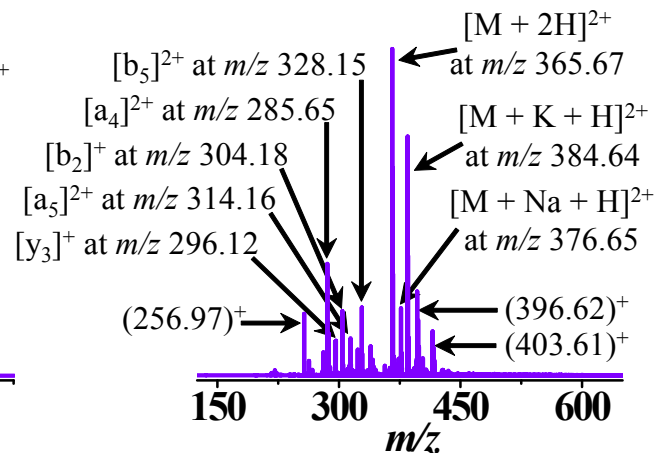


**Figure S1.** Representative low collision-energy IM profiles and mass spectra for pure solutions of either MGRYGF peptide (top, data represented in orange) or FRMYGG peptide (bottom, data represented in purple). The yellow rectangles in **(a)** and **(c)** are used to highlight the IM AT region from 2.08 ms to 3.18 ms that contains the doubly-charged precursor ion (*i.e.*,  $[M + 2H]^{2+}$ ). The MS data corresponding to highlighted IM regions in **(a)** and **(c)** were averaged to generate the extracted mass spectra (XMS) displayed in **(b)** and **(d)**, respectively. Labels are provided in **(a-d)** to indicate identities of peptide-related fragment ions. Parentheses are used in **(b)** and **(d)** to include  $m/z$ -values of unidentified ions.

was purchased from Bio-Rad (Hercules, CA, USA). DL-dithiothreitol (DTT, 98%), iodoacetamide (IAA, BioUltra, 99%) and ammonium bicarbonate (ABC, BioUltra, 99.5%) were obtained from Sigma-Aldrich (St. Louis, MO, USA). Sequencing grade modified trypsin was purchased from Promega (Madison, WI, USA). Ultrapure water with an overall ionic concentration of <0.1 ppb and a resistivity of ~18.2 MΩ·cm at 25 °C was produced in-house using either a Direct-Q 3 UV water purification system (EMD Millipore Corporation, Billerica, MA, USA). Optima grade methanol and acetic acid were purchased from Fisher-Scientific (Waltham, MA, USA). Ultracentrifugation cartridges (10 kDa cut-off) were obtained from PALL (Port Washington, NY, USA). Glass microscope slides (25×75 mm) were obtained from VWR (West Chester, PA, USA). Tris (50 mM) and ABC (10 mM) buffers were adjusted to pH values of 8.5 and 7.4, respectively.

Tissue samples were obtained from four-week-old breeding rats at the Louisiana State University School of Veterinary Medicine Division of Laboratory Animal Medicine (DLAM). All protocols for animal care and use were approved by the Institutional Animal Care and Use Committee at LSU and samples were handled as outlined by the Department of Environmental Health and Safety at BU. The animals were sacrificed by CO<sub>2</sub> (5 psi) exposure. Brain samples were collected, washed in 50 mM ammonium bicarbonate buffer for 30 seconds, and frozen in liquid nitrogen within 30 minutes. Frozen samples were stored at -80 °C. Thin sections were prepared with a Leica CM1850 cryostat (Leica Microsystems, Wetzlar, Germany) directly from the frozen tissue. Optimal cutting temperature (OCT) solution was used to fix one side of the sample to the cryostat support. Horizontal (transverse) rat brain sections were cut at a thickness of 50 μm, thaw-mounted on uncoated microscope slides, and stored at -80 °C.

Proteomic sample processing was performed at LSU as previously described.<sup>90</sup> Samples were collected into tubes and after addition of 500 μL of tris buffer (50 mM, pH 8.5), they were homogenized with a high-power ultrasonic homogenizer (Sonifier S-450, Emerson Electric, St. Louis, MO). Protein disulfide bond reduction was achieved by adding DTT to each tube to a final concentration of 10 mM. Samples were incubated at 80 °C for 45 minutes and, after cooling at room temperature for 15 minutes, transferred to ultrafiltration cartridges (with a molecular weight cutoff of 10 kDa) and centrifuged at 14,000 g for 20 minutes. Alkylation was performed by adding 100 μL of a 20 mM IAA solution to each unit followed by incubation in the dark for 30 minutes. After incubation, the samples were centrifuged again at 14,000 g for 10 minutes. Buffer exchanges and washing steps were performed by adding 100 μL of ABC buffer to each tube and centrifugation at 14,000 g for 10 minutes. This step was repeated twice, after which filter units were placed in clean tubes. Enzymatic digestion of the protein material was achieved using 50 μL of ABC buffer and 1 μL of a 50 ng/μL trypsin solution. Samples were incubated at 37 °C overnight and shaken at 200 rpm. After digestion, the filter units were centrifuged at 14,000 g for 10 min, 50 μL of ABC buffer added, and centrifuged again. The filter units were removed and the tryptic mixtures were vacuum dried. The centrifuge tubes containing the dried samples were packaged in dry ice and shipped to Baylor where they were stored at -40 °C before use.

Prior to MS analyses, dried samples were thawed and re-suspended in aqueous solutions containing 5% ACN and 0.1% FA. Based on a previous protocol,<sup>90</sup> sample concentration was estimated to be ~184 ng/ $\mu$ L. The re-suspended samples were vortexed for 30 seconds using a vortex mixer (VWR International, Radnor, PA) and centrifuged at 1,000 g for 1 minute using a microcentrifuge (Sorvall Legend Micro 21R, Thermo Scientific, Waltham, MA); the vortex/centrifuge step was repeated once.

### **HDMS<sup>E</sup> Data Acquisition**

The ultra-performance LC-MS/MS (UPLC-MS/MS) method was adapted from Geromanos *et al.*<sup>66</sup> Separation of tryptic peptides was performed using a UPLC system (nanoAcquity, Waters Corporation, Milford, MA) equipped with a Symmetry C18 pre-column (5  $\mu$ m, 20 mm  $\times$  180  $\mu$ m) and a BEH130 C18 analytical reversed-phase (RP) column (1.7  $\mu$ m, 100 mm  $\times$  100  $\mu$ m). Mobile phase solvents A and B were water and ACN, respectively (each with 0.1% formic acid (FA)). For each sample, a 4.0  $\mu$ L partial loop injection was transferred to the pre-column to desalt and pre-concentrate using 99% solvent A at a flow rate of 10  $\mu$ L min<sup>-1</sup> for 3 minutes. The pre-concentrated peptides were eluted to the analytical column and separated using a gradient of 5% to 45% solvent B at a flow rate of 600 nL min<sup>-1</sup>; a 60-minute and 15-minute separation were performed. Following separation, the mobile phase was ramped to 99% solvent B for 5 minutes and held at 99% solvent B for an additional 5-minutes. The mobile phase was ramped to 5% solvent B over 5 minutes, and the column was re-equilibrated at 5% solvent B for 15 minutes. Throughout the separation, the UPLC column temperature was held at 40 °C. The lock mass compound, [Glu<sup>1</sup>]-fibrinopeptide B (at a concentration of 300 fmol  $\mu$ L<sup>-1</sup>), was delivered at 500 nL min<sup>-1</sup> by the auxiliary pump of the UPLC system to the reference sprayer of the NanoLockSpray source of the mass spectrometer.

MS was performed in positive-ion mode ESI using a Synapt G2-S HDMS that was set to sensitivity mode (*i.e.*, V mode with a typical resolution of >10,000 FWHM). The TOF analyzer was externally calibrated using a sodium formate solution that yielded ions within the measured *m/z* window of 50 to 2000; all samples were measured in the same *m/z* range. The reference sprayer (containing [Glu<sup>1</sup>]-fibrinopeptide B at 300 fmol  $\mu$ L<sup>-1</sup>) was sampled every 30 seconds, and all TOF MS data were lock mass corrected (post acquisition) using the doubly-charged monoisotopic ions of [Glu<sup>1</sup>]-fibrinopeptide B at *m/z* 785.8426.

### **HDMS<sup>E</sup> Data Processing**

Raw HDMS<sup>E</sup> data were analyzed using ProteinLynx Global Server (PLGS Ver. 2.5.2; Waters Corporation) using the default processing parameters specific to HDMS<sup>E</sup> (*i.e.*, “Electrospray MS<sup>E</sup>” in PLGS). The processed data were searched against a UniprotKB/Swiss-Prot database<sup>91</sup> corresponding to the *rattus norvegicus* proteome (organism:“Rattus norvegicus (Rat) [10116]” AND proteome:up000002494, July 2016, 7,963 entries) appended with a one-time randomized version of the database using the following query parameters: precursor tryptic peptide tolerance of 5 ppm, fragment ion tolerance of 5 ppm, minimum fragment ion matches per peptide

set to 3, minimum fragment ion matches per protein set to 7, minimum peptide matches per protein set to 1, maximum protein mass set to 200,000,000 Da, trypsin was set as the primary digest reagent (no secondary digest reagent was used), 2 missed cleavages were allowed, fixed and variable modifications were set as carbamidomethyl C and oxidation M, respectively, and the false positive rate was set to 5.

### Improper Application of AIMD to Single Component IM Peaks

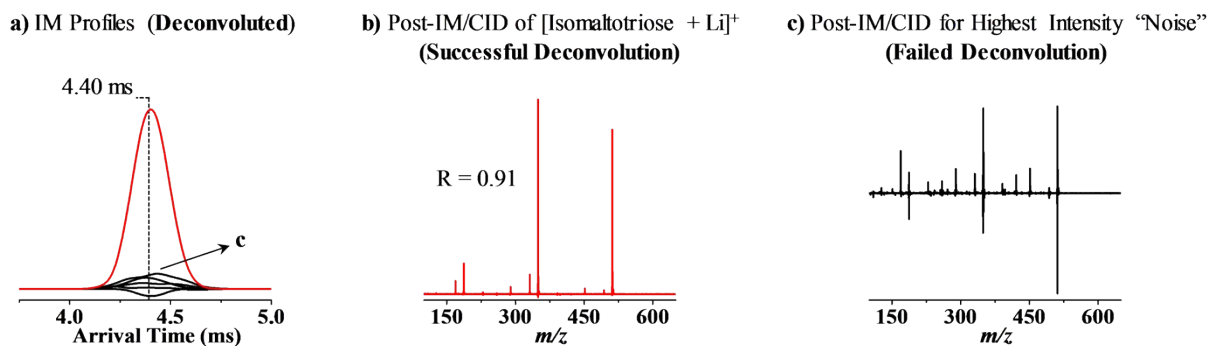


**Figure S2.** Six IM profiles generated by improper application of AIMD to a single component solution of isomaltotriose (a). As expected, AIMD successfully generated IM (red trace in (a)) and post-IM/CID (b) data for [isomaltotriose + Li]<sup>+</sup>. The remaining five black IM traces in (a) correspond to “non-real” (*i.e.*, noise) components. The non-real mass spectrum shown in (c) corresponds to the highest intensity noise component (arrow labeled with “c” in (a)).

Applying AIMD to single component IM peaks (mostly) yields erroneous IM profiles and mass spectra (Figure S2). Using the Malinowski factor indicator function<sup>92</sup> (previously integrated with AIMD<sup>11</sup>), it was determined that potentially six chemical “components” were present in a post-IM/CID MS dataset that corresponded to a single component solution of isomaltotriose (LiCl was added to solution for generated of Li-adducts). As expected, AIMD successfully deconvoluted the IM profile (Figure S2a, red trace with IM AT = 4.40 ms) and corresponding post-IM/CID mass spectrum (Figure 2Sb,  $R = 0.91$ ) for [isomaltotriose + Li]<sup>+</sup>. Also as expected, AIMD separated “non-real” (*i.e.*, noise) components (Figure S2a, black traces) from the real IM data of [isomaltotriose + Li]<sup>+</sup>. IM traces of “non-real” components generated by AIMD have (i) non-Gaussian shapes, (ii) >15% negative values, and/or (iii) >15% negative values in their corresponding MS data. As an example of “non-real” MS data generated by improper application of AIMD to single component IM peaks, the MS data corresponding to the highest intensity noise component (black IM trace in Figure S2a labeled as “c”) is shown in Figure S2c.

### Successful IM-MS Deconvolution of Components that have a 10x Concentration Difference

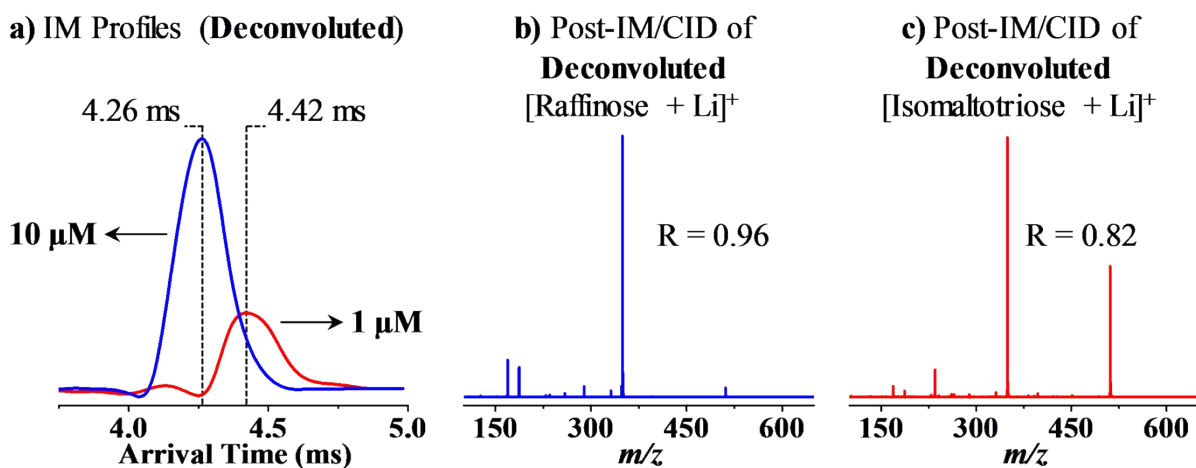


**Figure S3.** Broadband deconvolution was performed on IM-MS data of a solution containing 10  $\mu\text{M}$  [raffinose + Li]<sup>+</sup> and 1  $\mu\text{M}$  [isomaltotriose + Li]<sup>+</sup>. **(a)** Deconvoluted IM profiles for the two isomers and corresponding post-IM/CID mass spectra for **(b)** [raffinose + Li]<sup>+</sup> (blue) and **(c)** [isomaltotriose + Li]<sup>+</sup> (red)

Broadband IM-MS deconvolution was successfully performed on IM-MS data of a solution containing 10  $\mu\text{M}$  [raffinose + Li]<sup>+</sup> and 1  $\mu\text{M}$  [isomaltotriose + Li]<sup>+</sup> using a 45 V collision-energy and a data acquisition time of 1 minute (Figure S3). The deconvoluted IM ATs for [raffinose + Li]<sup>+</sup> (blue trace in Figure S3a with an IM AT = 4.26 ms) and [isomaltotriose + Li]<sup>+</sup> (red trace in Figure S3a with an IM AT = 4.40 ms) were within 1 IM bin of their corresponding single component validation sets, and the *R*-values were >0.70 for both isomers. When individually run as single component solutions, the IM peak ratio of [isomaltotriose + Li]<sup>+</sup> to [raffinose + Li]<sup>+</sup> was about 10%. The deconvoluted IM peak ratio of [isomaltotriose + Li]<sup>+</sup> to [raffinose + Li]<sup>+</sup> was about 30%.

The success of AIMD depends on the presence of detectable differences in post-IM/CID mass spectra as a function of IM bin number; many fragment ions generated *via* post-IM/CID of [raffinose + Li]<sup>+</sup> and [isomaltotriose + Li]<sup>+</sup> at the 45 V collision-energy have equivalent exact masses and comparable relative intensities. In cases where IM unresolved ions generate similar post-IM/CID fragment ions (*e.g.*, as for raffinose and isomaltotriose), it is more difficult for AIMD to detect differences in post-IM/CID mass spectra when the IM unresolved ions are present at significantly different concentrations (*i.e.*, one order of magnitude or greater). Nevertheless, broadband IM-MS deconvolution *via* AIMD was successful for a solution of 10  $\mu\text{M}$  [raffinose + Li]<sup>+</sup> and 1  $\mu\text{M}$  [isomaltotriose + Li]<sup>+</sup>.

## Background Species from Broadband Deconvolution of the Simulated Complex Mixture

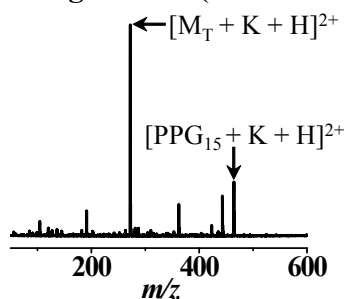
For the simulated complex mixture, broadband AIMD analysis of the IM AT region 2.08 ms to 3.18 ms allowed for deconvolution of the two hexapeptide isomers ( $[\text{MGRYGF} + 2\text{H}]^{2+}$  and  $[\text{FRMYGG} + 2\text{H}]^{2+}$  with orange and purple solid traces in Figure 6a, respectively) and nine additional background species (dotted traces for background species 1 to 9 in Figure 6a). Representative mass spectra from AIMD output for selected background species are displayed in Figures S4a-c (*viz.*, background species 5 (Figure S4a), 7 (Figure S4b), and 9 (Figure S4c)). The IM ATs for background species 5, 7, and 9 from AIMD output were 2.770 ms, 2.978 ms, and 3.185 ms, respectively. For comparison, counterpart mass spectra corresponding to these same three IM ATs were extracted from the data for simulated complex mixture (*i.e.*, each XMS corresponds to a single IM AT data point from the raw data) and are displayed in Figures S4d-f. Because mass spectra in Figure S4 were acquired at a 35 V collision-energy, observed ions include pseudo-molecular and fragment ions. Differences between AIMD output and extracted mass spectra are expected (and observed) because XMS from single data points (Figures S4d-f) are sums of all ions exiting the drift cell at a specified IM AT, whereas mass spectra from AIMD output correspond only to those ions that AIMD assigns to specific IM peaks (*i.e.*, specific background species).

Similarly, broadband AIMD analysis of the IM AT region 3.74 ms to 5.12 ms for the simulated complex mixture was utilized to deconvolute the two trisaccharide isomers ( $[\text{raffinose} + \text{Li}]^+$  and  $[\text{isomaltotriose} + \text{Li}]^+$  blue and red solid traces in Figure 7a, respectively) and ten additional background species (dotted traces for background species 1 to 10 in Figure 7a). Representative mass spectra from AIMD output for selected background species are displayed in Figures S5a-c (*viz.*, background species 2 (Figure S5a), 3 (Figure S5b), and 9 (Figure S5c)). The deconvoluted IM ATs for background species 2, 3, and 9 were 3.878 ms, 4.016 ms, and 5.055 ms, respectively. Counterpart mass spectra corresponding to these same three IM ATs were extracted from the data for the simulated complex mixture (*i.e.*, each XMS corresponds to a single IM AT data point from raw data) and are displayed in Figure S5d-f. As explained in the previous paragraph, the observed differences between mass spectra from AIMD output (Figures S5a-c) and XMS from the raw data (Figures S5d-f) were expected. In addition, observed common ions in AIMD output and XMS counterparts support the validity of the broadband IM deconvolution. Moreover, because AIMD does not use any curve fitting functions, Gaussian-like shapes of deconvoluted IM peaks further strengthen our confidence in broadband AIMD analysis as IM peak shapes conform to physical reality (Figure 7a).

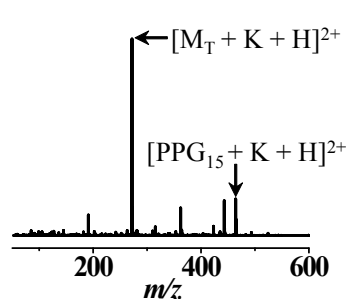
From AIMD Deconvolution at 35 V

From the Simulated Complex Mixture at 35 V  
(XMS from a single IM AT data point)

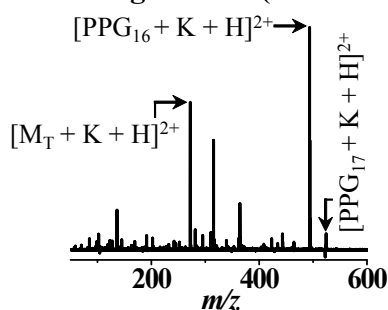
a) MS of background 5 (IM AT = 2.770 ms)



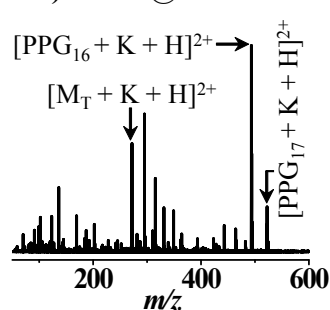
d) XMS @ 2.770 ms



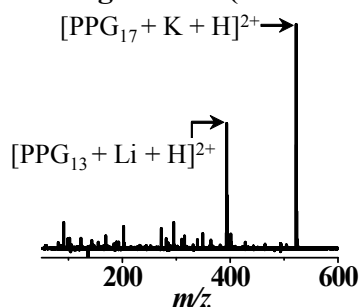
b) MS of background 7 (IM AT = 2.978 ms)



e) XMS @ 2.978 ms



c) MS of background 9 (IM AT = 3.185 ms)



f) XMS @ 3.185 ms

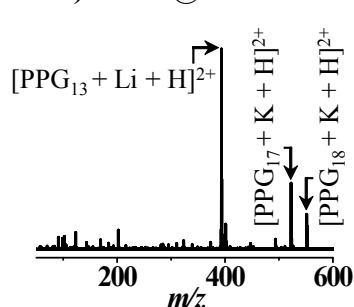
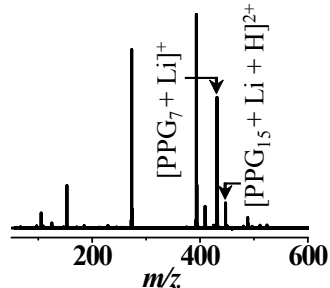


**Figure S4.** Representative mass spectra of background species present in the IM AT region 2.08 ms to 3.18 ms for the simulated complex mixture. Deconvoluted mass spectra of background species (a) 5, (b) 7, and (c) 9. Raw XMS corresponding to single IM AT data points of (d) 2.770 ms, (e) 2.978 ms, and (f) 3.185 ms. Data displayed in Figure S4 were collected using a 35 V collision-energy. Please refer to Figure 6a (main text) for deconvoluted IM profiles of background species 1 to 9.

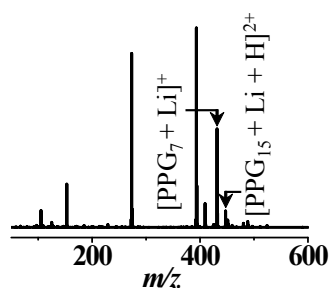
From AIMD Deconvolution at 35 V

From the Simulated Complex Mixture at 35 V  
(XMS from a single IM AT data point)

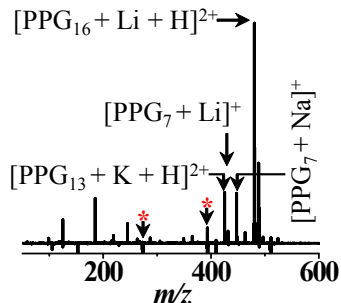
a) MS of background 2 (IM AT = 3.878 ms)



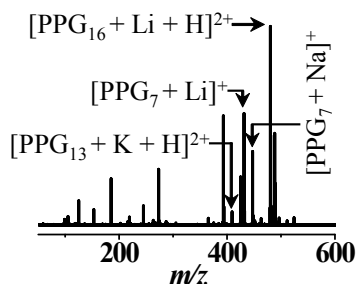
d) XMS @ 3.878 ms



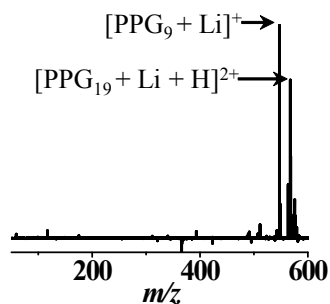
b) MS of background 3 (IM AT = 4.016 ms)



e) XMS @ 4.016 ms



c) MS of background 9 (IM AT = 5.055 ms)



f) XMS @ 5.055 ms

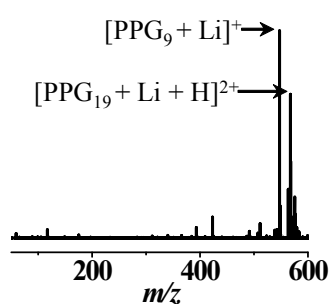


**Figure S5.** Representative mass spectra of background species present in the IM AT region 3.74 ms to 5.12 ms for the simulated complex mixture. Deconvoluted mass spectra of background species (a) 2, (b) 3, and (c) 9. Raw XMS corresponding to single IM AT data points of (d) 3.878 ms, (e) 4.016 ms, and (f) 5.055 ms. Data displayed in Figure S5 were collected using a 35 V collision-energy. The red asterisks at  $m/z$  273 and 393 in (b) signify negative relative intensity values that were  $> 15\%$  of the base peak intensity. Please refer to Figure 7a (main text) for deconvoluted IM profiles of background species 1 to 10.

## Comparison of Broadband and $m/z$ -isolated Approaches

The binary hexapeptide isomer mixture was freshly prepared, and serial dilutions were prepared at  $\sim 340$  nM,  $\sim 34$  nM, and  $\sim 3.4$  nM concentrations to compare the sensitivities of the  $m/z$  isolation<sup>27</sup> and broadband approaches. Broadband analysis of  $[M_P + 2H]^{2+}$  was re-performed on diluted samples according to the procedure described in the “Experimental” section. The settings for  $m/z$ -isolation of  $[M_P + 2H]^{2+}$  at  $m/z$  365 were identical to those used in a previous publication.<sup>27</sup> Except for the experimental settings used for ion isolation, identical experimental settings were utilized for broadband and  $m/z$ -isolated data acquisitions. Figures S6a and S6d represent convoluted IM and MS data collected *via*  $m/z$ -isolated and broadband data acquisitions, respectively. The base IM peaks at 2.42 ms in S6a and S6d correspond to the isomeric hexapeptide ions, and the inset post-IM/CID mass spectra in S6a and S6d are from corresponding  $m/z$ -isolated and broadband acquisitions, respectively. Deconvolution results for  $m/z$ -isolated (Figures S6b-c)

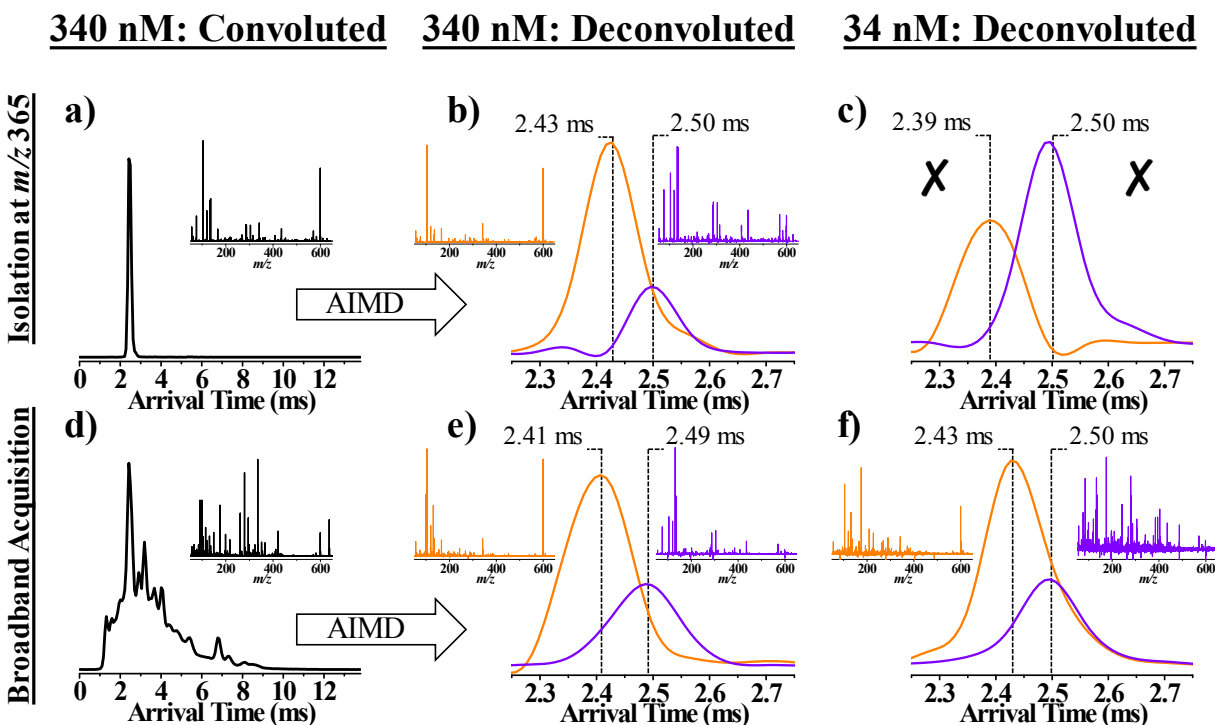


**Figure S6.** Sensitivity comparison of AIMD results obtained *via*  $m/z$ -isolated and broadband data acquisition. A 340 nM solution of MGRYGF and FRMYGG isomers was used to collect convoluted IM-MS data *via* (a)  $m/z$ -isolation of  $[M_P + 2H]^{2+}$  at  $m/z$  365 and (d) broadband data acquisition; the black IM profiles and inset mass spectra in (a) and (d) represent convoluted IM-MS data prior to deconvolution using AIMD. Results from deconvolution of (a) and (d) from the 340 nM solution *via* AIMD are represented in (b) and (e) respectively. The 340 nM solution was diluted to 34 nM (column 3), and AIMD results from this solution are shown in (c) and (f) for  $m/z$ -isolated and broadband data acquisitions, respectively. A black “X” is used to indicate “unacceptable results” in (c).

and broadband (Figures S6e-f) approaches are shown for the 340 nM (column 2) and 34 nM (column 3) solutions.

As discussed in the main text (section on “Comparison of Broadband and  $m/z$ -isolated Approaches”), including both throughput and multiplex advantages, broadband data acquisition provides a sensitivity enhancement of more than three orders of magnitude. For example, considering only the throughput advantage,<sup>75</sup> deconvolution using AIMD was 10 times more sensitive for broadband acquisition than for the  $m/z$ -isolated approach (see Figure S6). Both approaches allowed IM-MS deconvolution of the  $\sim 340$  nM solution. The  $m/z$ -isolated datasets had minimal IM and MS interference from unrelated ions, however, the  $m/z$ -isolation approach did not allow IM-MS deconvolution of the  $\sim 34$  nM or  $\sim 3.4$  nM (data not shown) hexapeptide isomer solutions. As the hexapeptide isomer concentration decreased, extracting accurate MS data from IM-MS data collected *via*  $m/z$ -isolation was unsuccessful because of insufficient product ion signal. Using  $m/z$ -isolation and a concentration of 34 nM (Figure S6c), the reconstructed MS data had abnormalities inconsistent with acceptable mass spectra (indicated by black “X” symbols in Figure S6c). Additionally, the relative intensity of the deconvoluted IM peaks in Figure S6c (*i.e.*, purple trace > orange trace) and the shape of the orange trace are inconsistent with the presented successful deconvolution of  $[M_p + 2H]^{2+}$ . However, AIMD assigned two groups of  $m/z$  values to two IM peaks with arrival times of 2.39 ms and 2.50 ms (orange and purple traces in Figure S6c, respectively).

Broadband analysis of the  $\sim 34$  nM isomer solution allowed successful IM-MS deconvolution of  $[MGRYGF + 2H]^{2+}$  and  $[FRMYGG + 2H]^{2+}$ . However, broadband analysis of the  $\sim 3.4$  nM solution was unsuccessful because AIMD did not output acceptable post-IM/CID mass spectra (please see “Data Analysis” section in main text for details on these requirements). Despite not yielding acceptable post-IM/CID mass spectra, broadband analysis of the  $\sim 3.4$  nM solution allowed AIMD assignment of two groups of  $m/z$  values to two IM peaks with drift times of  $\sim 2.40$  ms and  $\sim 2.50$  ms (not shown).

### **Comparison of UPLC Retention Times using 60 min and 15 min Separation**

We hypothesized that when analyzing the same sample using longer and shorter UPLC separations, the presence of IM-MS unresolved precursor ions could be determined by comparing peptide assignments from analyses of the longer and shorter UPLC separations; all peptide assignments in Figure S7 were made using ProteinLynx Global Server (PLGS) software. To examine the validity of our hypothesis, we utilized PLGS to process LC-IM-MS data from 60-minute and 15-minute UPLC separations using identical solvent ramps of 5% to  $\sim 45\%$  Solvent B for both runs. To identify potential IM-MS unresolved peptide ions, we tagged peptides that were assigned in the 60-min run but unassigned in the 15-min run. For example, PLGS processing of the 60-min UPLC run allowed successful characterization of VLSIGDGIAR (Figure S7a); however, this peptide was not assigned by PLGS in the 15-min UPLC run (Figure S7b). Figure S7 contains portions of selected ion chromatograms from HDMS<sup>E</sup> analysis of a rat brain whole tissue

digest that correspond to elution of VLSIGDGIAR and LIETYFSK peptides (blue and red traces in S7a, respectively). Using a 60-min UPLC separation, retention times of  $t_R = 21.98$  mins for LIETYFSK and  $t_R = 22.38$  for VLSIGDGIAR were sufficiently different for their successful

identification by PLGS. Upon careful examination of the IM and MS data for these peptides, it was confirmed that ions corresponding to these two peptides (*viz.*, [VLSIGDGIAR]<sup>2+</sup> and [LIETYFSK]<sup>2+</sup>), were IM-MS unresolved. For example, the closeness of experimentally measured ion mobility arrival times (*viz.*, 3.243 ms and 3.174 ms) and *m/z* values (500.7941 and 500.7725) for [VLSIGDGIAR]<sup>2+</sup> and [LIETYFSK]<sup>2+</sup> prevented successful PLGS assignment of VLSIGDGIAR using the dataset from the 15-min UPLC separation. The use of AIMD allowed successful deconvolution of IM profiles and post-IM/CID mass spectra of [VLSIGDGIAR]<sup>2+</sup> and [LIETYFSK]<sup>2+</sup> from the HDMS<sup>E</sup> dataset of the 15-min UPLC separation (for additional details, please refer to “Broadband Deconvolution of UPLC-HDMS<sup>E</sup> Proteomics Data” section within the main text).

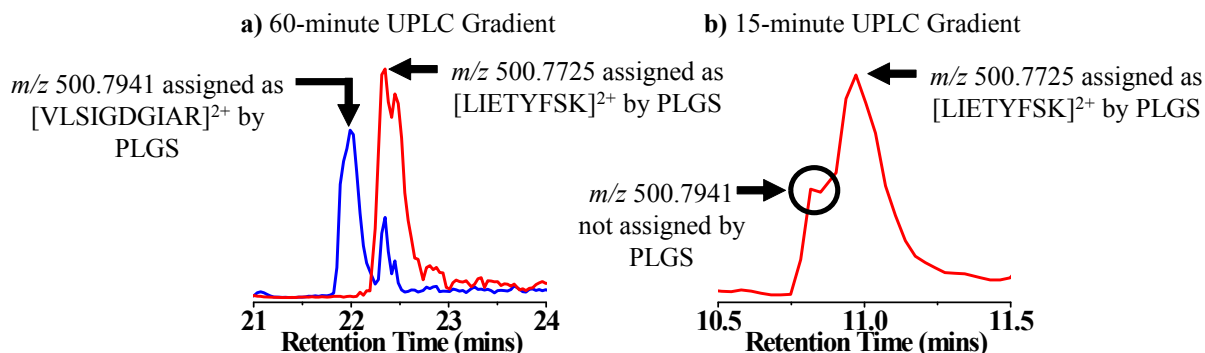


**Figure S7.** Representative UPLC chromatograms corresponding to small chromatographic windows from HDMS<sup>E</sup> analysis of a rat brain whole tissue digest using a (a) 60 minute and (b) 15 minute UPLC separation time. The peptides [VLSIGDGIAR]<sup>2+</sup> (blue) and [LIETYFSK]<sup>2+</sup> (red) are identified by PLGS using a 60 minute separation. Using a 15-minute separation, [VLSIGDGIAR]<sup>2+</sup> is UPLC unresolved and not identified by PLGS. The black circle in (b) indicates the unresolved elution of peptide VLSIGDGIAR.